A Low-Profile four-port MIMO Antenna for 5G-n79 Band with high diversity performance

Mohssine El Ouahabi[1], Aziz Dkiouak[1], Doae El Hadri[1], Alia Zakriti[1] and Mohamed Charif[2]

[1]Laboratory of Sciences and Advanced Technology, National School of Applied Sciences, Abdelmalek Essaâdi University, Tetuan, Morocc.

[2]Information and Telecommunication system Laboratory, Faculty of Sciences, Abdelmalek Essaadi University, Tetuan, Morocco.

Corresponding author: Mohssine El Ouahabi (moelouahabi@uae.ac.ma).

ABSTRACT This paper presents a simple design of a compact 4-port multiple-input multiple-output (MIMO) microstrip antenna using polarization diversity technique. The proposed structure consists of four monopole elements operating in the fifth generation n79 band (4800–5000 MHz). To achieve good performance with a more compact design, the four identical elements are arranged orthogonally to each other. The proposed antenna is fabricated using a Rogers RT6010 substrate with a compact size of 28 × 28mm^2 (0.46 λ_0* 0.46 λ_0), where λ_0 is the guided wavelength at the lowest generating frequency. The measured results of the manufactured antenna in terms of S-parameters and radiation pattern are in good agreement at the operating frequency band. Moreover, the diversity performance of the proposed MIMO antenna is evaluated through the envelope correlation coefficient (ECC), the diversity gain (DG), the total active reflection coefficient (TARC) and the channel capacity loss (CCL).

INDEX TERMS CCL, DG, diversity technique, ECC, MIMO antenna, n79.

I. INTRODUCTION

The fifth generation (5G) mobile communications systems are evolving rapidly to meet a wide range of demands, due to their advantages of high channel capacity, high spectral efficiency and massive connection density [1]. As one of the key technologies in 5G communication systems, MIMO technology exploits the use of multiple antennas at each end to improve performance reliability and thus allows for a linear increase in channel capacity without increasing bandwidth or transmission power. The diversity performance of a MIMO system is evaluated by studying important parameters such as ECC, DG, TARC and CCL. One of the main constraints of the MIMO technique is that the integration of multiple antennas in a small size increases the coupling in the structure and deteriorates the performance of the other parameters. In this regard, and to avoid these problems, several techniques have been introduced in the literature. Such as the insertion of Electromagnetic Band Gap structures (EBG) [2]–[4], Defected Ground Structure (DGS) [5]–[7], including the neutralization line [8]–[10], using metamaterial structures [11]–[13], and etching a slot in the feed lines [14], [15]. Other techniques have been proposed in the literature, which consist in inserting a parasitic element [16] or a meander-shaped resonator [17] between the radiating elements of MIMO antenna.

The objective of this work is to design a low profile of a compact MIMO antenna with a high performance using a substrate that is characterized by less loss (RT6010) and a polarization diversity technique. The evolution process of the presented antenna is studied based on the characteristics and optimized single-element antenna. To make antenna compact and achieve a polarization diversity without using any additional decoupling structures, each antenna element is arranged orthogonal to each other. The final 4-port MIMO antenna has the following advantages: compact size, high isolation, low envelope correlation coefficient and easy-to-fabricate structure.

II. INITIAL EVOLUTION PROCESS

The initial evolution process of the proposed MIMO antenna design, which contains three steps, is illustrated in fig.1.

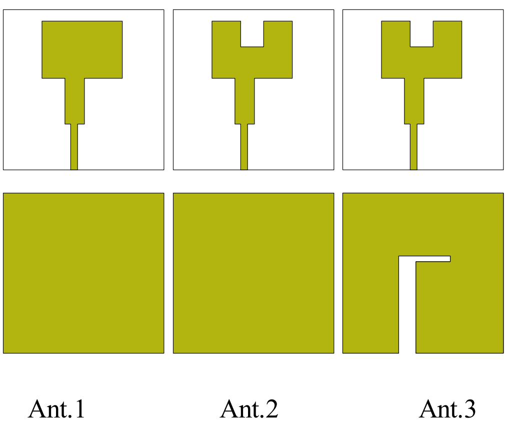

FIGURE 1. Design evolution of the compact MIMO antenna.

The first step (Ant.1) consists of a simple rectangular patch feeding with a quarter-wave transformer and a complete ground plane. The corresponding results of simulated S_{11} parameter of this step by using Computer Simulation Technology (CST) Microwave Studio Software are illustrated in fig.2. A resonant frequency at 5.54 GHz is generated with -7.2 dB.

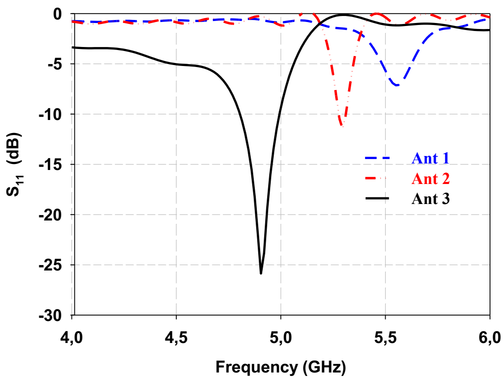

FIGURE 2. S_{11} parameter of the initial evolution process.

For the second and third steps (Ant.2 and Ant.3), respectively, the insertion of a rectangular slot in the radiating element and an inverted L-slot in the ground plane allowed the resonant frequency to be shifted towards the desired band and improved the S_{11} parameter (-26 dB). The result of the final antenna geometry (Ant.3) shows that the impedance bandwidth extends from 4.8 to 5 GHz.

III. DESIGN OF FOUR-PORT MIMO ANTENNA

The schematic of the proposed 4-port MIMO antenna design dimension is shown in fig.3, which illustrates how the proposed patch antennas are arranged in a limited space.

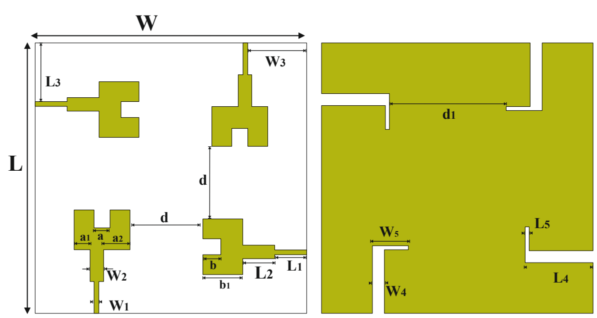

FIGURE 3. Proposed four-element MIMO antenna: (a) Front view, (b) Bottom view.

The presented antenna is printed on a Rogers RT6010 substrate (relative permittivity of 10.2, substrate thickness of 0.635 mm, and loss tangent of 0.0023). To make antenna compact and achieve polarization diversity without using any additional decoupling structures, each antenna element is arranged orthogonal to each other. The structure of the presented 4-port MIMO antenna with detailed dimensions is shown in fig.3 and the optimal values are presented in table 1.

TABLE I. Optimized antenna parameters

Parameters	W	W_1	W_2	W_3	W_4	W_5	h
Values (mm)	28	0.6	1.7	3.56	1.5	4.5	0.635
Parameters	L	L_1	L_2	L_3	L_4	L_5	b
Values (mm)	28	4	4	8.25	8.5	0.5	2.25
Parameters	b_1	a	a_1	a_2	d	d_1	
Values (mm)	5	2	2	3.3	4.6	10	

IV. EXPERIMENTAL RESULTS AND DISCUSSION

A. FABRICATION AND MEASUREMENT

In order to validate the simulated results, the proposed MIMO antenna is fabricated using the LPKF Protomat E33 machine. In addition, the S-parameters of the prototype MIMO antenna are measured by using a Rohde and Schwarz ZVB 20 vector network analyzer (fig.4).

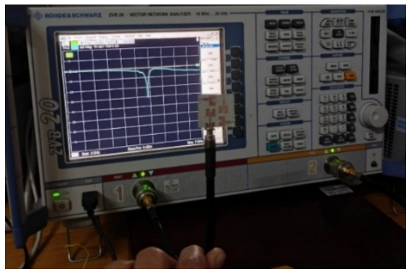

FIGURE 4. Proposed Antenna in the step of measuring the S parameters.

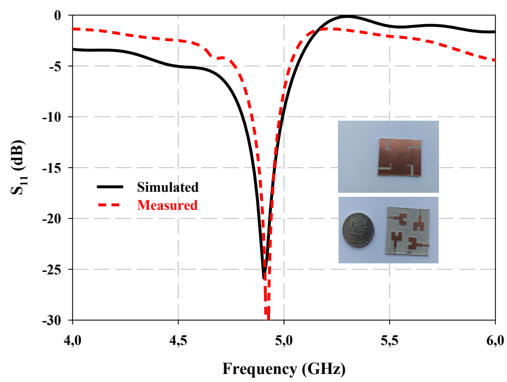

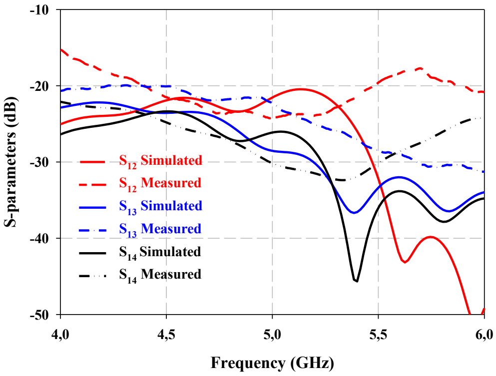

FIGURE 5. Simulated and Measured S-parameters S_{11}, S_{12}, S_{13} and S_{14}.

The measured and simulated results of the MIMO antenna are in good agreement (fig.5) and are summarized in Table 2.

TABLE II. Measured and simulated S-parameters of the proposed antenna.

Proposed MIMO antenna	F (GHz)	BW (GHz)	Isolation (dB)
Measured	4.93	4.83-4.98	-22.5
Simulated	4.9	4.8-5.0	-18.2

B. SURFACE CURRENT DISTRIBUTION

The surface current distribution at 4.9 GHz for the proposed MIMO antenna has been described to confirm the decoupling between the antenna elements. From the figure 6, we can see that the current density is highest around the rectangular slot in the radiating element and the inverted L slot in the ground plane, reaching a maximum of 424 A/m. Thus, there is no current distribution from antenna 1 to the other antennas and therefore little or no current transfer between the four elements, leading to a good isolation. This result is due to the techniques used in the construction of the proposed antenna, especially the diversity of polarization. In addition, at the edge of the excited patch and on the ground plane, the current has to bypass the slots, increasing the current path, which ultimately reduces the effect of mutual coupling and increases radiation efficiency at the frequency band (4.9 GHz).

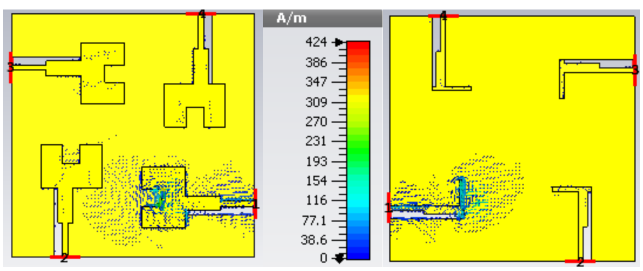

Figure 6. The surface current distribution of proposed MIMO antenna at 4.9 GHz

C. RADIATION PATTERN

The measured radiation patterns of the fabricated MIMO antenna are compared with the simulated patterns, as shown in fig.7 at the resonant frequency of 4.9 GHz.

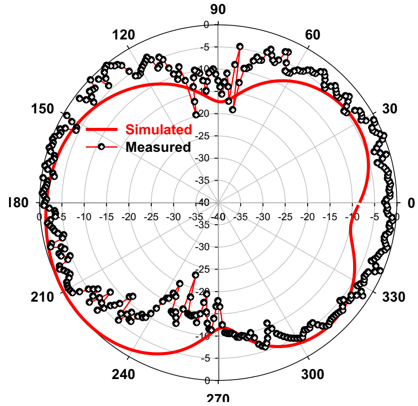

(a)

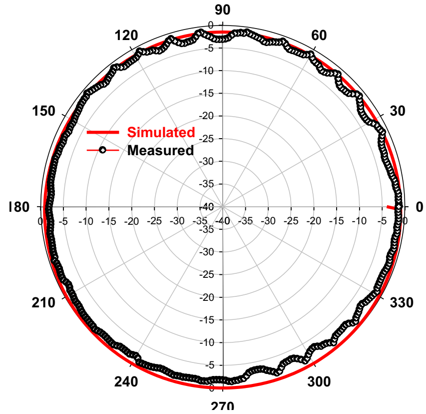

(b)

FIGURE 7. Simulated and measured radiation patterns at 4.9 GHz in the principal planes: (a) E-plane and (b) H-plane.

The radiation patterns in the H-plane are nearly omnidirectional, whereas they are identical to the radiation pattern of the dipole antenna in E-plane, which is quite suitable for fifth-generation applications. Because of symmetry, the measured results are obtained when one port is excited and other ports is terminated with a 50-ohm load.

The measured radiation patterns are mostly very similar to the simulated ones but there are some differences between them. This discrepancy is due to measurements that were not performed inside an anechoic chamber, but in a free space.

V. MIMO PERFORMANCE PARAMETERS

MIMO diversity performance can be explicated in terms of many parameters such as envelope correlation coefficient, diversity gain, total active reflection coefficient and channel capacity loss.

A. ENVELOPE CORRELATION COEFFICIENT AND DIVERSITY GAIN

The envelope correlation between the i^{th} and j^{th} antenna elements using far-field patterns [18] can be calculated from equation (1):

$$ECC_{(i,j)} = \frac{\left(\oint (X_{PR} E_{\theta i}(\Omega) E^*_{\theta j}(\Omega) P_{\theta}(\Omega) + E_{\varphi i}(\Omega) E^*_{\varphi j}(\Omega) P_{\varphi}(\Omega)) d(\Omega)\right)^2}{\oint (X_{PR} G_{\theta i}(\Omega) P_{\theta}(\Omega) + G_{\varphi i}(\Omega) P_{\varphi}(\Omega)) d(\Omega) \cdot \oint (X_{PR} G_{\theta j}(\Omega) P_{\theta}(\Omega) + G_{\varphi j}(\Omega) P_{\varphi}(\Omega)) d(\Omega)}$$

Where, X_{PR} denotes cross-polarization power ratio of the propagation environment. In the formula above, $G_{\theta}(\Omega) = E_{\theta}(\Omega)E^*_{\theta}(\Omega)$ and $G_{\varphi}(\Omega) = E_{\varphi}(\Omega)E^*_{\varphi}(\Omega)$ are the power patterns of θ and φ polarizations, respectively. $P_{\theta}(\Omega)$ and $P_{\varphi}(\Omega)$ denote the angular density functions of the θ and φ polarizations, respectively. $E_{\theta i}(\Omega)$ and $E_{\theta j}(\Omega)$ are the electric field patterns of the i^{th} and j^{th} antenna elements in the θ polarization, respectively. $E_{\varphi i}(\Omega)$ and $E_{\varphi j}(\Omega)$ are the electric field patterns of the i^{th} and j^{th} antenna elements in the φ polarization, respectively.

In the case of uniform multipath environment:

$$X_{PR} = 1 \text{ AND } P_{\theta}(\Omega) = P_{\varphi}(\Omega) = \frac{1}{4}$$

The envelope correlation coefficient for two antennas can be approximated as follow [18]:

$$ECC = \frac{\left(\oint \left(E_{\theta 1}(\Omega)E^*_{\theta 2}(\Omega) + E_{\varphi 1}(\Omega)E^*_{\varphi 2}(\Omega)\right) d(\Omega)\right)^2}{\oint \left(G_{\theta 1}(\Omega) + G_{\varphi 1}(\Omega)\right) d(\Omega) . \oint \left(G_{\theta 2}(\Omega) + G_{\varphi 2}(\Omega)\right) d(\Omega)}$$

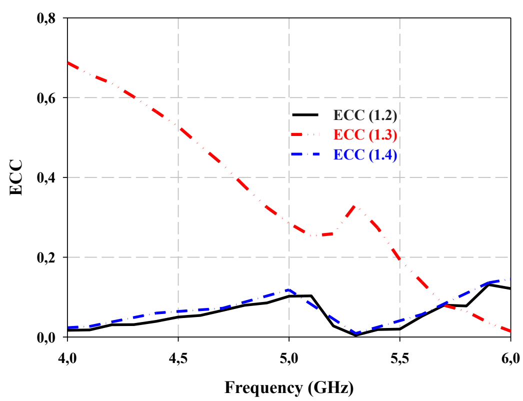

FIGURE 8. The ECC curve.

For a MIMO antenna system with four antenna elements (N= 4), the envelope correlations between the antennas i= 1 and j = 2, 3, 4 are shown in Fig.8, where ECC (1, 2), ECC (1, 3), and ECC (1, 4) are less than 0.31 which is good enough for MIMO applications.

The diversity gain is dependent on the correlation coefficient and can be given by the following approximate expression [19].

$$\mathrm{DG} = 10\sqrt{1 - |\rho|^2} \qquad (3)$$

Where ρ is the complex cross correlation coefficient, and $|\rho|^2 \approx$ECC

Fig.9 illustrates the simulated diversity gain of proposed MIMO antenna. These curves show that the diversity gain from the far-field patterns is about 9.2 dB at the operating frequency.

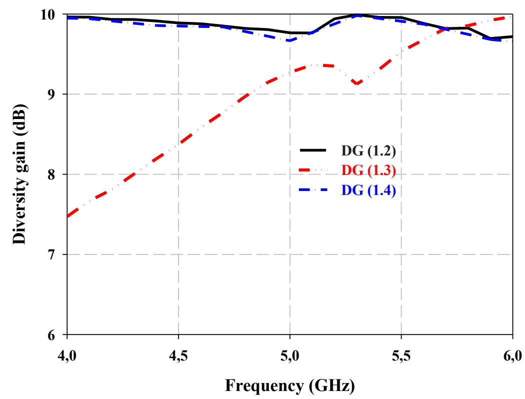

FIGURE 9. The DG curve.

B. TOTAL ACTIVE REFLECTION COEFFICIENT AND CHANNEL CAPACITY LOSS

TARC is calculated using the S-parameters [20] of MIMO antenna using the following equation.

$$TARC = \frac{\sqrt{\sum_i^N |b_i|^2}}{\sqrt{\sum_i^N |a_i|^2}} \qquad (4)$$

Where a_i and b_i is the incident wave and reflected wave respectively. TARC is less than −10 dB at the 5G n79 band as depicted in fig.10 (a).

The simulated TARC coefficient of the proposed MIMO antenna is less than -10 dB at the frequency band, which is required for good MIMO performance. The channel capacity loss has been included among the MIMO performance parameters, thereby providing details of channels capacity losses of the system during the correlation effect. The CCL is calculated numerically by the following equations.

$$CCl = -\log_2 det(\psi^R) \qquad (5)$$

Where ψ^R is the correlation matrix

$$\psi^R = \begin{bmatrix} \rho_{11} & \cdots & \rho_{1j} \\ \vdots & \ddots & \vdots \\ \rho_{i1} & \cdots & \rho_{ij} \end{bmatrix}$$

$$\rho_{ii} = 1 - \left|\sum_{n=1}^{M} S^*_{in} \times S_{ni}\right| \; and \; \rho_{ij} = -\sum_{n=1}^{M} S^*_{in} \times S_{nj}$$
$$for\ i,j = 1,2 \ldots M$$

ρ_{ii} and ρ_{ij} are the correlation coefficients.

In general, it is desirable to have a CCL value less than 0.4 bits/s/Hz [21] at the frequency band. As shown in fig.10 (b), the CCL is very well at 4.9 GHz and its value is less than 0.05 bit/s/Hz.

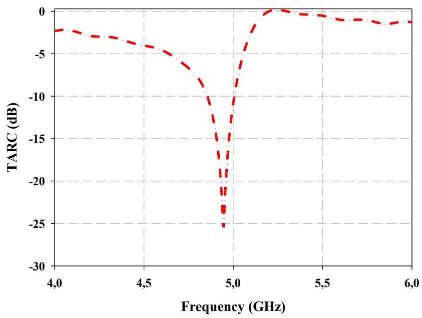

(a)

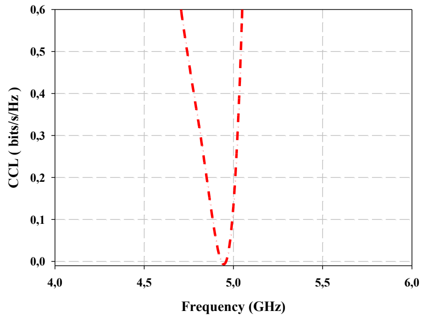

(b)

FIGURE 10. (a): TARC and (b): CCL

VI. PERFORMANCE COMPARISON

Table 3 summarizes the comparison between the proposed antenna and the other antennas reported in the literature.

TABLE III. Performance comparison between proposed structure and other MIMO antennas

Ref. N°	Size (mm^2) (λ_0)	MIMO elements	Frequency (GHz)	Minimum Isolation (dB)	ECC
[22]	80 × 80 $0.12\lambda_0$*$0.12\lambda_0$	5	4.5–5.0	15	0.01
[23]	80 × 80 $0.94\lambda_0$*$0.94\lambda_0$	4	3.5/5.5	18	<0.2
[24]	30 × 30 $0.48\lambda_0$* $0.48\lambda_0$	4	4.8–6.0	10	<0.15
[25]	112 × 112 $1.93\lambda_0$* $1.93\lambda_0$	4	5.15/5.3	22	<0.15
[26]	70 × 70 $0.12\lambda_0$* $0.12\lambda_0$	4	2.5/ 5.5	21	<0.27
[27]	56×56 $0.93\lambda_0$* $0.93\lambda_0$	4	4.9	20	<0.01
[28]	40 × 40 $0.63\lambda_0$* $0.63\lambda_0$	4	4.7–5.1	25	<0.01
P.S	28 × 28 $0.46\lambda_0$* $0.46\lambda_0$	4	4.9	-18.2	< 0.31

P.S= Proposed Structure

It can be observed that the presented antenna has advantages over existing antennas in terms of size and the techniques used. As well as the performances of our antenna such as ECC and DG are calculated from the far field.

VII. CONCLUSION

This paper presented a simple design of a rectangular antenna with an inverted L-shaped defected ground structure. The proposed antenna was designed to resonate at the resonance frequency of 4.9 GHz allocated for the 5G n79 band. Furthermore, the proposed antenna has been developed as a four-element MIMO array system arranged orthogonally to each other, which yields a minimum isolation of 18.2 dB. In order to verify the presented idea, a prototype of the developed antenna was manufactured and measured. According to the measured results, the proposed antenna covers the frequency band from 4.83 to 4.98 GHz. The ECC, DG, TARC and CCL of the proposed MIMO antenna are also taken into account, giving excellent results for MIMO applications.

ACKNOWLEDGMENT

This work was partially supported by Faculty of Sciences, under Information Systems and Telecommunications Laboratory, Abdelmalek Essaadi University, Tetuan, Morocco, Supervised by Professor Mohsine Khalladi

REFERENCES

[1] K. M. Mak, H. W. Lai, K. M. Luk, and C. H. Chan, “Circularly polarized patch antenna for future 5G mobile phones,” IEEE Access, vol. 2, pp. 1521–1529, 2014, doi: 10.1109/ACCESS.2014.2382111.

[2] W. Wu, B. Yuan, and A. Wu, “A quad-element UWB-MIMO antenna with band-notch and reduced mutual coupling based on EBG structures,” Int. J. Antennas Propag., vol. 2018, 2018, doi: 10.1155/2018/8490740.

[3] N. Kumar and U. K. Kommuri, “MIMO antenna mutual coupling reduction for WLAN using spiro meander line UC-EBG,” Prog. Electromagn. Res. C, vol. 80, pp. 65–77, 2018, doi: 10.2528/pierc17101601.

[4] A. K. Biswas and U. Chakraborty, “Reduced mutual coupling of compact MIMO antenna designed for WLAN and WiMAX applications,” Int. J. RF Microw. Comput. Eng., vol. 29, no. 3, pp. 13–20, 2019, doi: 10.1002/mmce.21629.

[5] J. Banerjee, A. Karmakar, R. Ghatak, and D. R. Poddar, “Compact CPW-fed UWB MIMO antenna with a novel modified Minkowski fractal defected ground structure (DGS) for high isolation and triple band-notch characteristic,” J. Electromagn. Waves Appl., vol. 31, no. 15, pp. 1550–1565, 2017, doi: 10.1080/09205071.2017.1354727.

[6] B. T. P. Madhav, Y. Usha Devi, and T. Anilkumar, “Defected ground structured compact MIMO antenna with low mutual coupling for automotive communications,” Microw. Opt. Technol. Lett., vol. 61, no. 3, pp. 794–800, 2019, doi: 10.1002/mop.31626.

[7] A. Dkiouak, A. Zakriti, M. El Ouahabi, N. A. Touhami, and A. Mchbal, “Design of a Four-Element MIMO Antenna with Low Mutual Coupling in a Small Size for Satellite Applications,” Prog. Electromagn. Res. M, vol. 85, pp. 95–104, 2019, doi:10.2528/PIERM19071202.

[8] A. K. Biswas and U. Chakraborty, “Investigation on decoupling of wide band wearable multiple-input multiple-output antenna elements

using microstrip neutralization line," Int. J. RF Microw. Comput. Eng., vol. 29, no. 7, pp. 1–11, 2019, doi: 10.1002/mmce.21723.

[9] A. Kayabasi, A. Toktas, E. Yigit, and K. Sabanci, "Triangular quad-port multi-polarized UWB MIMO antenna with enhanced isolation using neutralization ring," AEU - Int. J. Electron. Commun., vol. 85, pp. 47–53, 2018, doi: 10.1016/j.aeue.2017.12.027.

[10] S. Zhang and G. F. Pedersen, "Mutual Coupling Reduction for UWB MIMO Antennas with a Wideband Neutralization Line," IEEE Antennas Wirel. Propag. Lett., vol. 15, pp. 166–169, 2015, doi: 10.1109/LAWP.2015.2435992.

[11] M. EL Ouahabi, A. Zakriti, M. Essaaidi, A. Dkiouak, and H. Elftouh, "A miniaturized dual-band MIMO antenna with low mutual coupling for wireless applications," Prog. Electromagn. Res. C, vol. 93, pp. 93–101, 2019, doi: 10.2528/PIERC19032601.

[12] A. Iqbal, O. A. Saraereh, A. Bouazizi, and A. Basir, "Metamaterial-based highly isolated MIMO antenna for portable wireless applications," Electronics, vol. 7, no. 10, pp. 3–10, 2018, doi: 10.3390/electronics7100267.

[13] S. Luo, Y. Li, Y. Xia, G. Yang, L. Sun, and L. Zhao, "Mutual coupling reduction of a dual-band antenna array using dual-frequency metamaterial structure," Appl. Comput. Electromagn. Soc. J., vol. 34, no. 3, pp. 403–410, 2019.

[14] L. S. Yahya, K. H. Sayidmarie, F. Elmegri, and R. A. Abd-Alhameed, "Arc-shaped monopole antennas with reduced coupling for WLAN and WIMAX applications," 2017 Internet Technol. Appl. ITA 2017 - Proc. 7th Int. Conf., pp. 218–223, 2017, doi: 10.1109/ITECHA.2017.8101942.

[15] L. S. Yahya, K. H. Sayidmarie, F. Elmegri, and R. A. Abd-Alhameed, "Crescent-shaped double-monopole antennas with reduced coupling for WLAN and WIMAX applications," 2015 Internet Technol. Appl. ITA 2015 - Proc. 6th Int. Conf., pp. 393–398, 2015, doi: 10.1109/ITechA.2015.7317434.

[16] Z. Li, Z. Du, M. Takahashi, K. Saito, and K. Ito, "Reducing mutual coupling of MIMO antennas with parasitic elements for mobile terminals," IEEE Trans. Antennas Propag., vol. 60, no. 2, pp. 473–481, 2012, doi: 10.1109/TAP.2011.2173432.

[17] J. Ghosh, S. Ghosal, D. Mitra, and S. R. B. Chaudhuri, "Mutual coupling reduction between closely placed microstrip patch antenna using meander line resonator," Prog. Electromagn. Res. Lett., vol. 59, pp. 115–122, 2016, doi: 10.2528/PIERL16012202.

[18] J. Zhang, J. Ouyang, K. Z. Zhang, and F. Yang, "A novel dual-band MIMO antenna with lower correlation coefficient," Int. J. Antennas Propag., vol. 49, no. 10, pp. 2636–2647, 2012, doi: 10.1155/2012/512975.

[19] M. Schwartz, W. R. Bennett, and S. Stein, "Communication systems and techniques," McGraw-Hill, New York, pp. 470–474, 1966.

[20] M. S. Sharawi, "Book Reviews : Book Reviews," Print. MIMO Antenna Eng. Artech House Norwood, MA, USA, 2014., doi: 10.1177/001316447503500129.

[21] H. Shin and J. H. Lee, "Capacity of multiple-antenna fading channels: Spatial fading correlation, double scattering, and keyhole," IEEE Trans. Inf. Theory, vol. 49, no. 10, pp. 2636–2647, 2003, doi: 10.1109/TIT.2003.817439.

[22] R. K. Jaiswal, K. Kumari, A. K. Ojha, and K. V. Srivastava, "Five-port MIMO antenna for n79-5G band with improved isolation by diversity and decoupling techniques." J. Electromagn. Waves Appl., vol. 36, no. 4, pp. 542–556, 2021, doi: 10.1080/09205071.2021.1975315.

[23] A. K. Dwivedi, A. Sharma, A. K. Singh, and V. Singh, "Design of dual band four port circularly polarized MIMO DRA for WLAN / WiMAX applications," J. Electromagn. Waves Appl., vol. 34, no. 15, pp. 1990–2009, 2020, doi: 10.1080/09205071.2020.1801522.

[24] M. Yang and J. Zhou, "A compact pattern diversity MIMO antenna with enhanced bandwidth and high-isolation characteristics for WLAN / 5G / WiFi applications," Microw. Opt. Technol. Lett., vol. 62, no. 06, pp. 2353–2364, 2020, doi: 10.1002/mop.32334.

[25] G. Das, N. K. Sahu, A. Sharma, R. K. Gangwar, and M. Sharawi, "FSS Based Spatially Decoupled Back to Back Four Port MIMO DRA with Multi-directional Pattern Diversity," IEEE Antennas Wirel. Propag. Lett., vol. 18, pp. 15552–1556, 2019, doi: 10.1109/LAWP.2019.2922276.

[26] L. Malviya, R. K. Panigrahi, and M. V Kartikeyan, "A 2 × 2 Dual-Band MIMO Antenna with Polarization Diversity for Wireless Applications," Prog. Electromagn. Res. C, vol. 61, pp. 91–103, 2016, DOI: 10.2528/PIERC15110401.

[27] S. Sharma and M. Kumar, "Design and Analysis of a 4-Port MIMO Microstrip Patch Antenna for 5G Mid Band Applications," Prog. Electromagn. Res. C, vol. 129, no. 2022, , pp. 231–243, 2023, doi:10.2528/PIERC22120104.

[28] H. Ali et al., "Four-Port MIMO Antenna System for 5G n79 Band RF Devices," Electronics, vol. 11, no. 1, p. 35, 2022, doi: 10.3390/electronics11010035.